5th International Conference on Control Engineering&Information Technology (CEIT-2017)
Proceeding of Engineering and Technology –PET
Vol.34 pp.33-37

# Design and Control of Biomechanical Leg for Enhanced Human-like Walking

Zaier Riadh[#1], Omer ElDirdiry [*2], Mohamed A. Sayari [#3]
[*1,2] *College of Engineering, Sultan Qaboos University, Muscat, Oman*
[1]zaier@squ.edu.om
[*3] *Electromechanical Systems Laboratory (LASEM),*
*National Engineering School of Sfax University of Sfax,– Tunisia*

***Abstract*— This paper presents a design and control of a biomechanical leg that is capable to mimic the human walking. The leg has to possess the major features of the human gait. The design of this leg is being manufactured in the Mechanical Lab in Sultan Qaboos University. The mechanical structure of the biomechanical leg is made of very light materials mainly, aluminum and carbon fiber parts. The control of the biomechanical leg is made such that the Van der Pol oscillator represents the closed loop control system. The controlled plant is modelled as a cart-inverted pendulum system, which results in a non-linear controller. By tuning the parameter of the controller, the closed loop system will exhibit a stable limit cycle that can be demonstrated by the phase plot of the measured zero moment point using the force sensor located under the sole plate of the leg. The robustness of the controller against plant uncertainty is discussed throughout simulation results.**

***Keywords*— Van der Pol oscillator, biomechanical leg, passive joint, human-like dynamic, locomotion, gait, toe joint**

## I. Introduction

During the few last decades, the fields of biomechanics and robotics have seen a significant development in the designs and control of the biomechanical legs and prostheses. Several studies have focused on building legged robots that mimic human motions [1]. There are two types of legged robots; powered and passive legs. In this study, the powered robotic leg will be considered, where its joints are driven with electric actuators. In contrast, the passive legs rely on the force of gravity to rotate the joints. Under certain condition, such that the angle of ground slope, it can perform a stable gait [2,3].

The main motivation behind the design and control of the biomechanical leg is to build an experimental platform that can facilitate the study of pathological gaits due to a number of causes such as foot drop problem. Inline with this context, the biomechanical leg to be designed has to possess the main features of a human leg.

On the other hand, controlling legged-robot locomotion can be thought of as a complex problem, which is difficult to solve with too many parameters that are hard to tune. Conventional controllers based on neural networks suffer less flexibility in both, the implementation, and the tuning of the neurons' connections weights. The idea of coupling a simple nonlinear controller with a controlled plant and ending up with a Van der Pol oscillator is considered in this paper. This fascinating idea in dealing with the locomotion problem has already been approached by some researchers such as in [4][5]. Yet, their implementations on biped robots, as well as its robustness have not been discussed. Other locomotion controllers based on a nonlinear oscillator, termed central pattern generator (CPG), have been developed [6][7][8][9]. Although significant progress has been made using small numbers of tightly coupled neurons, those approaches have some limitations in implementing and adapting them to a changing environment. For instance, the stability of a walking robot requires controlling many joints, and thus, too many parameters of the coupled oscillators will need tuning [10]. Some trials towards simplification of locomotion pattern generator have been conducted [11][12] using piecewise linear oscillators. The research framework in [11] is based on piecewise linear functions that shape the locomotion pattern using recurrent neural network and sensory feedback. Although the method provides a comprehensive knowledge about the robot dynamics and allows easy implementation of sensory feedback and much flexibility to include reflexes capability to the humanoid robot, the locomotion controller includes too many neurons and connecting wires with weights hardly tuned. The work in [12] deals with the phase response properties of Matsuoka's oscillator, which has been interpreted as a piecewise linear oscillator with phase resetting control.

In this paper, we will introduce the Van der Pol oscillator as a closed loop control system that includes both the plant and the corresponding feedback controller. The plant will consist of a cart-inverted pendulum system, which is a simplified model of the humanoid robot. As a result, a nonlinear feedback controller will be obtained. The inputs to the controller are the velocity and position of the zero moment point (ZMP) of the cart-inverted pendulum. The parameters of the controller will be tuned so that the closed loop system will exhibit a stable limit cycle. The robustness of the controller against plant uncertainty and time-varying delay feedback signals will be discussed throughout simulation results.

In this paper, section 2 will describe the design of the biomechanical leg. Section 3 will introduce the biomechanical behavior and human walking gaits. In section 4, the control of the leg based on Van der Pol oscillator. Section 5 presents the


ISSN 2356-5608

5th International Conference on Control Engineering&Information Technology (CEIT-2017)
Proceeding of Engineering and Technology –PET
Vol.34 pp.33-37

simulation results and discussion. Lastly, a summary is presented in Section 6.

## II. Mechanical Design

In this section, the design and the components used to build the biomechanical leg are described (Fig. 1).

### A. *Dimensions, Weights, and Joints Range Motions*

TABLE I and TABLE II compare the average dimensions and weights of human-legs, for 100 voluntaries form the study [13] with the proposed design of the biomechanical leg.

TABLE I: Dimensions Comparison in (m)

| Symbol | Human Leg[18] | Biomechanical Leg |
|---|---|---|
| L1 | 0.41 | 0.41 |
| L2 | 0.44 | 0.44 |
| L3 | 0.26 | 0.26 |
| H1 | 0.09 | 0.09 |
| H2 | 0.05 | 0.04 |
| H3 | 0.07 | 0.06 |

TABLE II: Weights Comparison in (kg)

| Segment | Human Leg | Biomechanical Leg |
|---|---|---|
| Thigh | 10 | 0.98 |
| Shank | 3.1 | 0.31 |
| Foot | 1.0 | 1.41 |
| Toe | - | 0.36 |

Fig. 1. An Isometric View for the Two Biomechanical Legs Designed with Solidworks.

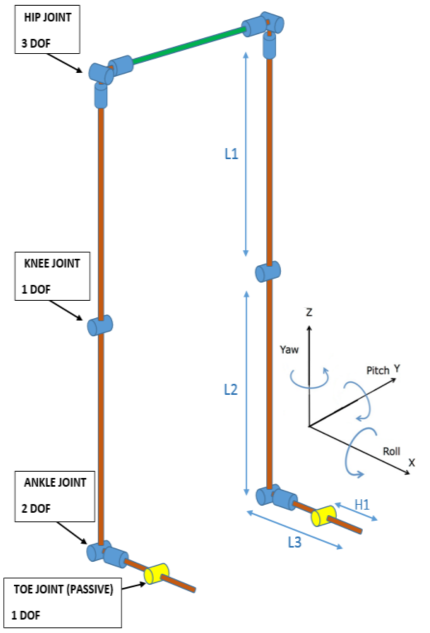


Fig. 2. The Kinematic Parameters of the Biomechanical Legs.

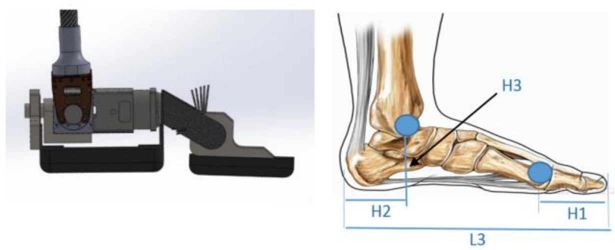


(a) (b)

Fig. 3. Side Views for (a) the Biomechanical Foot and (b) a Sketch of Human Foot.

The dimensions were selected in the design to be as close as possible to the human leg, in order to make it easier to mimic the human gaits (Fig. 2). However, the weight was selected to be as light as possible, so that it will be easier for us to add weights if needed. For this purpose, mainly, aluminium and carbon fibre materials were used to build this design. The dimensions L1, L2, and L3 are referred to the lengths of the thigh, the shank, and foot, respectively.

To study the foot motion in more details, the dimensions H1, H2, and H3 (Fig. 3) are referred to some segments in the foot part of human leg. Moreover, the lengths of the biomechanical leg have to be similar to lengths of the human leg, as depicted in TABLE I. However, the weight of the biomechanical leg will not be a pivotal issue in order to mimic the human motion, as long as the motors are capable of carrying the body segments and performing the gait.

The study [13] was considered to determine the proportionality of heights and the weights for our designed segments. The averages of the total body height and weight are selected from [13] which are 173.1 cm and 73 Kg, respectively. Hence, the percentage of height and the weight of the leg segments with respect to the total height and weight of the body are found to be; for the heights: thigh 23.2%,

5th International Conference on Control Engineering&Information Technology (CEIT-2017)
Proceeding of Engineering and Technology –PET
Vol.34 pp.33-37

shank 24.7%, and foot 4.25%, and for the weights: thigh 14.16%, shank 4.33%, and foot 1.37%.

Based on these percentages, the heights and the weights of the human leg segments are calculated and documented in TABLE I and TABLE II. The actual heights and weights for the biomechanical leg segments, after building the design, are given in the same tables. The weights of the thigh and shank of the biomechanical leg are very light compared to the human leg segments. This is due to the very light materials what are used to build the biochemical leg. Although, very light materials are used to design the biomechanical leg, the foot segment is slightly heavier than the foot segment for the human foot, as shown in TABLE II. This is due to the complicated design and large number of parts that are used to build the foot segment in our design. Many studies contributed in calculating the average joints-range motion of human, e.g. [14]. The joints ranges for the human right leg, taken from [14], is compared to the joints ranges of the biomechanical leg in TABLE III. The joints ranges of the biomechanical leg were calculated based on the motion capability of the joints (not causing any collapses) in the CAD design in Solidworks. Notice that the joints ranges of human leg are within the ranges of motion of the biomechanical leg except in the knee (pitching) and the ankle (pitching). Even though, all these recorded joints ranges of the biomechanical leg are enough to perform the normal human walking.

An easy way to comply with the conference paper formatting requirements is to use this document as a template and simply type your text into it.

### *B. Motors Selection*

As shown in Figure 2, which describes the kinematic parameters and the motors locations of the biomechanical leg, three motors, 3-Degree of Freedom (DOF), are used in the hip position, for pitching, rolling and yawing motions. The ankle joint is represented by 1 DOF pitching motion, whereas 2 DOF are used in the knee joint to perform the rolling and pitching motions. The toe joint (the only passive joint in this structure) is represented by 1 DOF without any actuator. TABLE IV shows the maximum joints torque values (done by our research group in MATLAB) that are required to accomplish normal human gate. DYNAMIXEL PRO motors, provided by [15] are used in our design since they can provide the sufficient torque values to perform the gain. From TABLE IV, it is clear that the pitching movement required more torque than the rolling and yawing movements. The motor L42-10-S300-R (DYNAMIXEL PRO motor) was selected to represent the low torque joints, whereas the motor L54-30-S400-R was selected to fulfil the high toque joint (the pitching hip joint and the pitching knee joint, which are required maximum torque of 5.23 Nm and 6.35 Nm, respectively). The specification for these two motors are shown in Figure 5. Another major factor was considered in the selection of these motors, which is the angular speed of motors that is required to mimic the normal speed of the joints for the human while walking in a normal gate. Since human angular velocity for a normal joint is, approximately, 20 rpm [16] which is equal to 120 degree per second, these two motors were selected so that they can perform well in this speed.

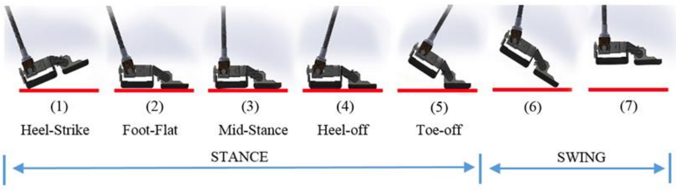


Fig. 4. A Simulation of one biomechanical leg during the stance and swing phases of a normal gait.

## III. Biomechanical Behavior and Human Walking Gaits

In order to mimic the human motion, by the designed biomechanical leg it is important to study the cyclic pattern of the human motion. The step is the base of this cyclic behavior and it consists of two phases: the stance phase, which represent about 60% of the duration of the whole step, and the swing phase, which take approximately the remaining 40% [8].

Fig. 4 highlights phases of one step, presented by our designed biomechanical leg. As shown in the figure, in the beginning of the step, the heel part of the biomechanical foot strikes the ground. The bottom part of the leg was made of a rubber material in order to absorb the shock when the heel hits the ground. Then, the pitching motor, in the ankle joint, rotates causing a flat foot orientation, on the ground level. After that, with the help of the upper structure of the biomechanical leg, the ankle joint pitches in the opposite direction to reach the mid-stance phase of the foot and continues its rotation to reach the heel-off phase. Because of this motion, the heel part of the foot will start to rise, from the ground level, while the toe part maintains its level on the ground. As a result, the passive joint in the toe stores some energy, in a spring element, see Section 5. In the end of the stance phase, and the beginning of the swing phase, the spring element will start to release its stored energy. Consequently, the toe part will start to rise from the ground level. During the swing motion, the ankle pitching motor will return to its original orientation so that the foot become ready for a new stance phase. It is worth mentioning that during this cyclic motion, the upper motors (in the hip and the knee joints) contribute to help the foot part to maintain the right orientation to perform the stance and the swing motions.

## IV. Control method of the Biomechanical

In this section, we introduce the Van der Pol oscillator as a closed loop control system that includes both the plant and the corresponding feedback controller (Fig. 5).

### *A. Rolling Motion Control Using Van der Pol Oscillator*

Knowing that one of the oscillators that can exhibit stable limit cycle is the Van der Pol Oscillator, which can be described by a second order nonlinear differential equation (1), could be regarded as a mass-spring-damper system.

$$\ddot{x} + \mu(x^2 - 1)\dot{x} + x = f(t)\,, \tag{1}$$

where $\mathbf{x}$ and $\dot{\mathbf{x}}$ are the states of the system and $\mu$ is a control parameter that represents the degree of nonlinearity of the system or its damping strength. The function *f*(t) represents the input to the system that can be regarded as a feedback control. Since the idea in this study is to have the closed loop control system behaves as the Van der Pol oscillator, the plant may be viewed as a cart-inverted pendulum system, which is a simplified model of the humanoid robot, which will lead to a nonlinear feedback controller. The inputs to the controller are the velocity and position of the zero moment point (ZMP) of the cart-inverted pendulum. The control input can be expressed as follow.

$$u = -x(1 + l/g) + \mu(1 - x^2)\dot{x}, \tag{2}$$

where $l$ is the height of the center of mass of the inverted pendulum and $g$ is the gravity constant. The parameters of the controller $\mu$ can be tuned so that the closed loop system will exhibit a stable limit cycle. The linear model of the plant with the control input can be expressed by the following ordinary differential equation.

$$\ddot{x} - (l/g)x = u, \tag{3}$$

The robustness of the controller against plant uncertainty and time-varying delay feedback signals is discussed in the following section simulation.

## V. Simulation Results and Discussion

For $\mu = 0.5$, the system exhibits a stable limit cycle as shown in Fig, 6. The convergence speed to the limit cycle can be faster or slower if this parameter is increased or decreased, respectively. However this parameter must change within the stability margin, i.e., the system must have a stable limit cycle. On the other hand, the controller (2) can be modified to have more degree of freedom as follows.

$$u = -x(x + l/g) + \mu(\lambda - x^2)\dot{x}, \tag{4}$$

where $\lambda$ is the second parameter that modulate the amplitude of the system output. In other words, it can change the amplitude of the rolling motion. To investigate the robustness of the controller we introduced small perturbation to the system and the resultant limit cycle is shown in Fig. 7, which shows that there are stable limit cycles that stays within a basin of attraction.

To change the frequency of frequency of the Van der pol oscillator, we can modify (1) to be as follows.

$$\ddot{x} + \mu(x^2 - \lambda)\dot{x} + \omega^2 x = f(t), \tag{5}$$

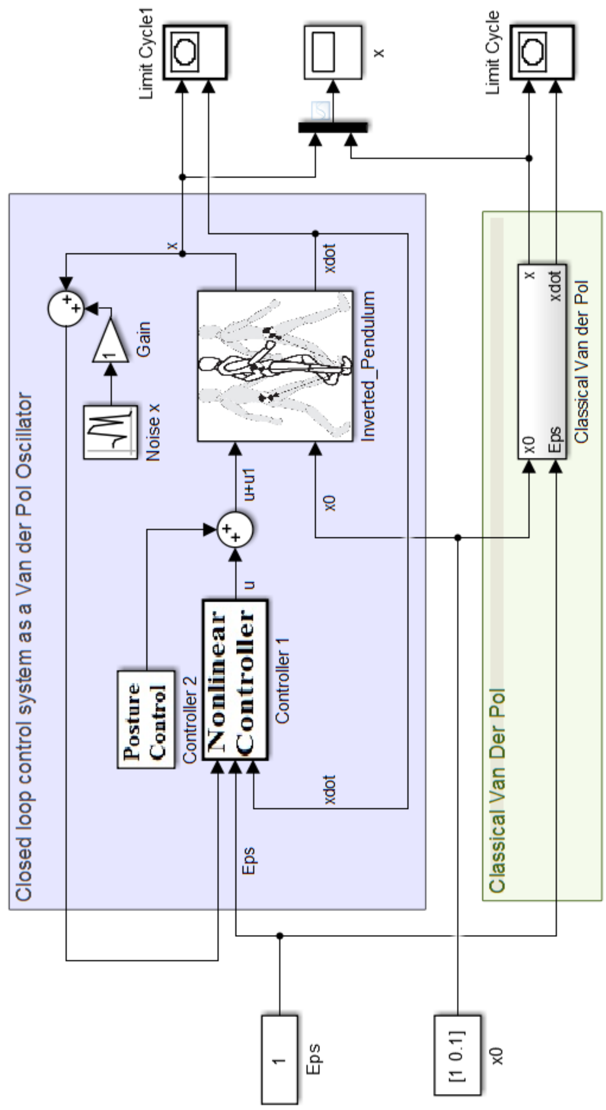


Fig. 5 Overall control system of the Humanoid robot using Van der Pol Oscillator

where $\omega = 4\pi^2/T^2$ and $T$ is the gait duration. According to (5), the control input (2) can be modified as follows.

$$u = -x(\omega^2 + l/g) + \mu(\lambda - x^2)\dot{x}, \tag{6}$$

Fig. 8 and Fig. 9 shows the case when T= 1s and T=6.28 s, respectively.

## VI. Conclusions

This study presented the design procedure for biomechanical legs with a passive toe joint. The design was made based on the motion capability of normal human gait where the joints' ranges of human joints are considered. The design of these biomechanical legs was made from very light materials. The dimensions of the designed leg and the motors

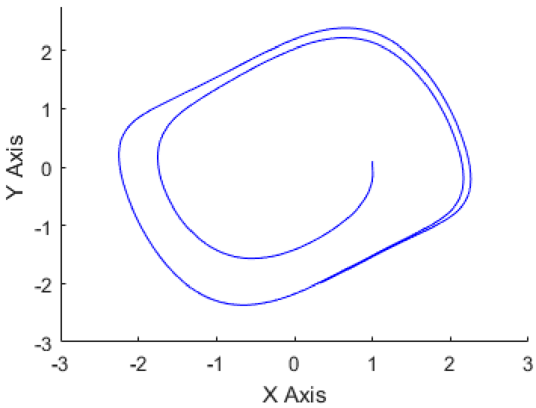


Fig. 6 Phase portrait showing the limit cycles when $\mu = 0.5$ (x axis represents x and Y axis represents $\dot{x}$ )

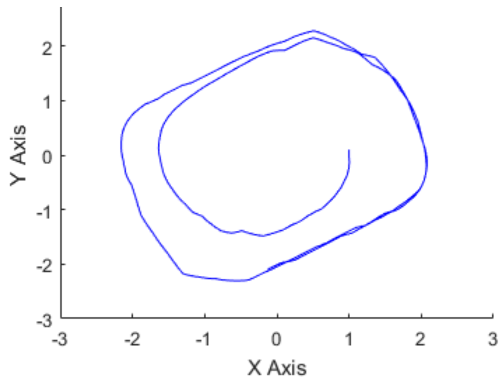


Fig. 7 Phase portrait showing the limit cycles when μ=0.5and in the presence of random noise affecting the value of x (normally distributed random noise with variance =0.1)

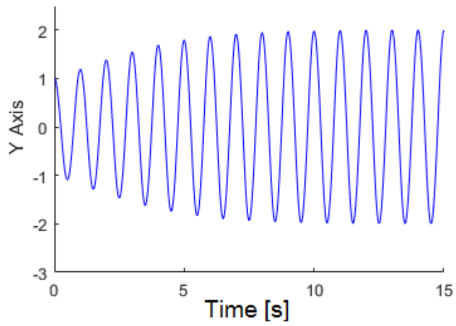


Fig. 8 The output plot of x when *T*=1s

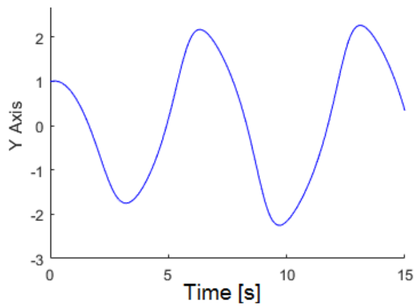


Fig. 9 The output plot of x when *T*=6.28s

of the joints were selected so that the biomechanical leg could mimic the gait of normal human. On the other hand, the control of the leg was made based on the Van der Pol oscillator, which represents the closed loop system. The Controller performance was demonstrated through simulation results. It was shown that in the presence of plant disturbance, the system can still exhibit a stable motion. Moreover, the controller could be modified to include two parameters in addition the convergence rate parameter μ; one parameter λ to control the rolling amplitude and a scond one ω to modulate the frequency of the rolling motion (i.e., the gate). Experimental result will be conducted soon on Darwin-Op2 humanoid robot. The robot dynamics coupled with this controller through sensory system is expected to show natural looking motion.

## ACKNOWLEDGMENT

The authors acknowledge The Research Council of Oman for their financial support of this study.

## REFERENCES

[1] Denny, Joe, Mohamed E, Shannon Angel D, Royson DD (2016), Humanoid Robots–Past, Present and the Future. *European Journal of Advances in Engineering and Technology* 3(5): 8-15.

[2] Collins, Steven H, Wisse M, Ruina A (2001), A three-dimensional passive-dynamic walking robot with two legs and knees. *The International Journal of Robotics Research* 20(7): 607–15

[3] McGeer, Tad (1990), Passive dynamic walking. *The international Journal of Robotics Research* 9(2): 62–82.

[4] M. Attilio. Time Delay Control for Two van der Pol Oscillators. Journal of Computational and Nonlinear Dynamics, 6, 1, pp. 011016, 2011.

[5] F.M. Atay. Van der Pol's oscillator under delayed feedback. Journal of Sound and Vibration 218, 2, 333{339, 1998.

[6] N. Jiangsheng, H. Seiji and K. Atsuo. A Model of Neuro–Musculo–Skeletal System for Human Locomotion Under Position Constraint Condition. The Journal of Biomechanical Engineering, 125, 4, 499{506, 2003.

[7] M. Marilyn. Central Pattern Generation of Locomotion: A Review of the Evidence. The Journal of the American Physical Therapy, 82, 1, 69{83, 2002.

[8] K. Matsuoka. Sustained oscillations generated by mutually inhibiting neurons with adaptation. The Journal of Biological Cybernetics, 52, 367{376, 1985.

[9] K. Seo, S. Chung and J.J. Slotine. CPG-based control of a turtle-like underwater vehicle. Autonomous Robots, 28, 3, 247{269, 2010.

[10] A. Kale, G. Salunke, K. Kadam, and M. Jagdale. CPGs Inspired Adaptive Locomotion Control for Hexapod Robot. The International Journal of Engineering Science Invention. 2, 4, 2319{ 6734, 2013.

[11] R. Zaier and S. Kanda. Piecewise-Linear Pattern Generator and Reflex System for Humanoid Robots. IEEE Int. Conf. on Robotics and Automation. 2188{2195, 2007.

[12] K. Nakada, Y. Sato and K. Matsuoka. Tuning Time Scale Parameter of Piecewise Linear Oscillators for Phase Resetting Control. The 21st Annual Conference of the Japanese Neural Network Society. 2011

[13] P. De Leva. (1996). "Adjustments to Zatsiorsky-Seluyanov's segment inertia parameters," J. Biomech., vol. 29, no. 9, pp. 1223–1230.

[14] R. Grasso, M. Zago, and F. Lacquaniti. (2000). "Interactions between posture and locomotion: motor patterns in humans walking with bent posture versus erect posture," J. Neurophysiol., vol. 83, no. 1, pp. 288–300.

[15] "Robotis.com, (2016). DYNAMIXEL PRO, [Online]. Available: http://en.robotis.com/index/index.php. [Accessed: 10- Oct- 2016]."

[16] R. Riemer and A. Shapiro. (2011). "Biomechanical energy harvesting from human motion: theory, state of the art, design guidelines, and future directions," J. Neuroeng. Rehabil., vol. 8, no. 1, p. 1.